Acta Mech
DOI 10.1007/s00707-012-0619-y

Jan Awrejcewicz · Valeriy Storozhev · Vladimir Puzyrev

Controlling the dynamic behavior of piezoceramic cylinders by cross-section geometry

Received: 8 October 2011

Abstract This paper focuses on the possibilities of controlling the dispersion spectra and wave characteristics of cylindrical waveguides by changing their geometry and electro-elastic properties. We consider cylinders with classical circular and hollow cross-sections, and waveguides that have sector cut of arbitrary angular measure in the cross-section. Numerical results are presented for the cylinders of all studied types with different boundary conditions. It is shown that the required wave characteristics can be obtained by a variation of the cross-section geometry of the waveguides.

1 Introduction

Piezoelectric ceramic materials are widely used in diverse applications such as sensor systems and signal processing. Their wide application range has motivated various studies of wave propagation in piezoceramic waveguides. Descriptions of the piezoelectric effect and fundamentals for the modeling of the dynamic behavior of piezoelectric components are given, in particular, in classical works of Tiersten [1], Berlincourt et al. [2], Maugin [3], and Parton and Kudryavtsev [4]. Many applications of piezoelectric devices are described by Uchino [5,6], Benes et al. [7], and Drinkwater and Wilcox [8]; additional references can be found in some recent articles [9–12].

Methods to analyze free harmonic waves propagating in elastic cylinders were developed long ago, and investigations [13–19] should be mentioned among the important works in the field. These and other notable contributions made before the mid-1960s are described in detail by Meeker and Meitzler [20]; some later works are enlightened by McNiven and McCoy [21], and Thurston [22]. The paper of Zemanek [23] should be mentioned separately since the author presented the frequency equation describing waves of all types of

J. Awrejcewicz · V. Puzyrev
Department of Automatics and Biomechanics, Technical University of Lodz,
1/15 Stefanowskiego Str., 90924 Lodz, Poland
E-mail: awrejcew@p.lodz.pl

V. Storozhev · V. Puzyrev (✉)
Department of Mathematics, Donetsk National University, 24 Universitetskaya Str., 83001 Donetsk, Ukraine
E-mail: vladimir.puzyrev@gmail.com
Tel.: +38-067-6293135
Fax: +38-062-3054628

V. Storozhev
E-mail: stvi@i.ua

V. Puzyrev
Department of Computer Applications in Science and Engineering,
Barcelona Supercomputing Center, c/ Gran Capita, 2-4, 08034 Barcelona, Spain

Published online: 25 February 2012

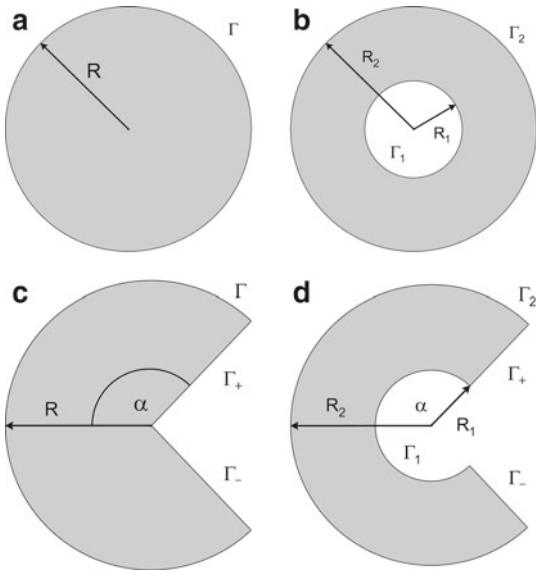

Fig. 1 Cross-sections of the waveguides

modes and gave a detailed review of the behavior of complex-valued roots (this work was first presented as a dissertation in 1962 and was published only 10 years later [24]).

In the past decades, the problem of elastic wave propagation in noncircular finite and infinite cylinders and related problems has received a great deal of attention [25–36]. At the same time, active use of piezoelectric devices in various applications has been continuously increasing, stirring up the interest in modeling of dynamic behavior of piezoelectric components, in particular, of cylindrical geometry. Studies on elastic cylinders have provided a strong foundation for the analysis of piezoelectric waveguides, though these problems are more difficult since elastic and electric field parameters are coupled through the constitutive relations of piezoelectricity.

The dynamic behavior of piezoelectric cylinders has been studied from different points of view [37–50]. A modern historical outline of the development of these problems and their applications in electro-mechanical devices can be found in [46,48]. Problems for piezoceramic cylinders with simple geometries were solved with the analytical solutions that satisfy exactly the boundary conditions. In [53], the authors studied wave propagation in hollow piezoceramic cylinders of sector cross-section and obtained the dispersion equations that satisfy the boundary conditions on the cylindrical and flat surfaces. More complex geometries and multiple layers numerical approaches, especially finite element method (FEM), were used both for elastic [28,32,34] and piezoelectric [45,50] waveguides. Nevertheless, a limited amount of investigations exists on the wave propagation problems in noncircular piezoelectric cylinders.

In this work, we study how the specific wave properties can be achieved by variation of the waveguide's cross-section. The paper is organized as follows. In Sect. 2, the problem under consideration and its solution approach are introduced. The equations of motion of the piezoelectric cylinder are analytically integrated. In Sect. 3, we consider different types of boundary conditions, and frequency equations that exactly satisfy them are derived in Sect. 4 for all four types of cylinders under consideration. Numerical calculations of the real and imaginary branches of the dispersion spectra, phase and group velocities of nonaxisymmetric electroelastic waves, and discussion are presented in Sect. 5.

2 Formulation of the problem

Figure 1 illustrate the types of cross-section geometry of waveguides under consideration: cylinders with classical circular (a) and hollow (b) cross-sections, and cylinders with the sector cut of arbitrary angular measure in circular (c) and hollow (d) cross-sections.

Governing equations for piezoelectric materials include the three-dimensional equations of motion and quasistatic Maxwell's equations, which in terms of a cylindrical coordinate system can be expressed as

$$\frac{\partial \sigma_{rr}}{\partial r} + \frac{1}{r}\frac{\partial \sigma_{r\theta}}{\partial \theta} + \frac{\partial \sigma_{rz}}{\partial z} + \frac{\sigma_{rr} - \sigma_{\theta\theta}}{r} = \rho \ddot{u}_r,$$

$$\begin{aligned}
\frac{\partial \sigma_{r\theta}}{\partial r}+\frac{1}{r}\frac{\partial \sigma_{\theta\theta}}{\partial \theta}+\frac{\partial \sigma_{\theta z}}{\partial z}+\frac{2\sigma_{r\theta}}{r}&=\rho\ddot{u}_{\theta},\\
\frac{\partial \sigma_{rz}}{\partial r}+\frac{1}{r}\frac{\partial \sigma_{\theta z}}{\partial \theta}+\frac{\partial \sigma_{zz}}{\partial z}+\frac{\sigma_{rz}}{r}&=\rho\ddot{u}_{z},\\
\frac{\partial D_r}{\partial r}+\frac{1}{r}\frac{\partial D_{\theta}}{\partial \theta}+\frac{\partial D_z}{\partial z}+\frac{D_r}{r}&=0;
\end{aligned} \tag{1}$$

and the constitutive relations for a piezoelectric material with axial polarization

$$\begin{aligned}
\sigma_{rr}&=c_{11}S_{rr}+c_{12}S_{\theta\theta}+c_{13}S_{zz}-e_{13}E_z,\\
\sigma_{\theta\theta}&=c_{12}S_{rr}+c_{11}S_{\theta\theta}+c_{13}S_{zz}-e_{13}E_z,\\
\sigma_{zz}&=c_{13}S_{rr}+c_{13}S_{\theta\theta}+c_{33}S_{zz}-e_{13}E_z,\\
\sigma_{r\theta}&=2c_{66}S_{r\theta},\quad \sigma_{rz}=2c_{44}S_{rz}-e_{15}E_r,\quad \sigma_{\theta z}=2c_{44}S_{\theta z}-e_{15}E_{\theta},\\
D_r&=2e_{15}S_{rz}+\varepsilon_{11}E_r,\quad D_{\theta}=2e_{15}S_{\theta z}+\varepsilon_{11}E_{\theta},\\
D_z&=e_{13}S_{rr}+e_{13}S_{\theta\theta}+e_{33}S_{zz}+\varepsilon_{33}E_z;
\end{aligned} \tag{2}$$

where $\sigma_{\alpha\beta}$, $S_{\alpha\beta}$ are, respectively, the dimensionless components of stress and strain; u_{α}, E_{α}, and D_{α} are the dimensionless components of displacement, electric field intensity, and electrical displacement; c_{ij}, e_{ij}, and ε_{ij} denote the elastic, piezoelectric, and dielectric constants, respectively; ρ is the mass density.

The strains and electrical field components are related to displacements and electrical potential φ by [51]

$$\begin{aligned}
S_{rr}&=\frac{\partial u_r}{\partial r},\quad S_{\theta\theta}=\frac{1}{r}\frac{\partial u_{\theta}}{\partial \theta}+\frac{u_r}{r},\quad S_{zz}=\frac{\partial u_z}{\partial z},\\
S_{r\theta}&=\frac{1}{2}\left(\frac{1}{r}\frac{\partial u_r}{\partial \theta}+\frac{\partial u_{\theta}}{\partial r}-\frac{u_{\theta}}{r}\right),\quad S_{rz}=\frac{1}{2}\left(\frac{\partial u_r}{\partial z}+\frac{\partial u_z}{\partial r}\right),\\
S_{\theta z}&=\frac{1}{2}\left(\frac{\partial u_{\theta}}{\partial z}+\frac{1}{r}\frac{\partial u_z}{\partial \theta}\right);\\
E_r&=-\frac{\partial \varphi}{\partial r},\quad E_{\theta}=-\frac{1}{r}\frac{\partial \varphi}{\partial \theta},\quad E_z=-\frac{\partial \varphi}{\partial z}.
\end{aligned} \tag{3}$$

We seek the solutions of the problem for harmonic waves with angular frequency ω and wavenumber k traveling along the axial direction of a cylinder:

$$\begin{aligned}
\mathbf{u}&=\mathrm{Re}\left(\mathbf{u}^{(0)}(r,\theta)\cdot \mathrm{e}^{-i(\omega t-kz)}\right),\\
\varphi&=\mathrm{Re}\left(\varphi^{(0)}(r,\theta)\cdot \mathrm{e}^{-i(\omega t-kz)}\right).
\end{aligned} \tag{4}$$

In order to solve the system of partial differential equations (1), we use wave potentials method, which was introduced by Buchwald [52] and later has been used by many other authors [19,26,33,35,48]. These potential functions ψ_j are related to displacement components as

$$u_r^{(0)}=\frac{\partial \psi_1}{\partial r}+\frac{1}{r}\frac{\partial \psi_4}{\partial \theta},\quad u_{\theta}^{(0)}=\frac{1}{r}\frac{\partial \psi_1}{\partial \theta}-\frac{\partial \psi_4}{\partial r},\quad u_z^{(0)}=\psi_2,\quad \varphi^{(0)}=\psi_3. \tag{5}$$

After a series of transformations described in [53], potential functions ψ_j take the form

$$\psi_p=\sum_{j=1}^{3}\beta_{pj}\chi_j(r,\theta)\quad p=\overline{(1,3)},\quad \psi_4=\chi_4(r,\theta). \tag{6}$$

Here, $\chi_j(r,\theta)$ are the metaharmonic functions

$$\nabla^2\chi_j(r,\theta)+\gamma_j^2\chi_j(r,\theta)=0\quad j=\overline{(1,4)}; \tag{7}$$

γ_1^2, γ_2^2, γ_3^2 are the roots of the bicubic algebraic equation and β_{pj} are described in [53]; $\gamma_4^2=\frac{\Omega^2-c_{44}k^2}{c_{66}}$, where Ω is the normalized angular frequency.

Functions $\chi_j(r,\theta)$ are chosen below in the well-known form of Bessel functions of the first and second kind and sin/cos functions. Their specific representation depends on the problem to be solved.

3 Boundary conditions

Several boundary conditions can be chosen depending on the problem being considered. For circular cylinders without cuts (C-waveguides), we consider two types of boundary conditions: the stress-free cylindrical surface

$$(\sigma_{rr})_\Gamma = (\sigma_{r\theta})_\Gamma = (\sigma_{rz})_\Gamma = 0; \tag{8.1}$$

and the displacement-fixed cylindrical surface

$$(u_r)_\Gamma = (u_\theta)_\Gamma = (u_z)_\Gamma = 0. \tag{8.2}$$

The surface is considered as covered by thin short-circuited electrodes with potential equal to zero (close circuit condition)

$$(\varphi)_\Gamma = 0. \tag{9}$$

Another electric boundary condition, the open-circuit condition $(D_r)_\Gamma = 0$, could also be applied in the model.

For hollow cylinders without cuts (H-waveguides), the inner cylindrical surfaces can be also stress-free

$$(\sigma_{rr})_{\Gamma_1} = (\sigma_{r\theta})_{\Gamma_1} = (\sigma_{rz})_{\Gamma_1} = (\varphi)_{\Gamma_1} = 0, \tag{10.1}$$

or displacement-fixed

$$(u_r)_{\Gamma_1} = (u_\theta)_{\Gamma_1} = (u_z)_{\Gamma_1} = (\varphi)_{\Gamma_1} = 0; \tag{10.2}$$

as well as the outer one

$$(\sigma_{rr})_{\Gamma_2} = (\sigma_{r\theta})_{\Gamma_2} = (\sigma_{rz})_{\Gamma_2} = (\varphi)_{\Gamma_2} = 0, \tag{11.1}$$

or

$$(u_r)_{\Gamma_2} = (u_\theta)_{\Gamma_2} = (u_z)_{\Gamma_2} = (\varphi)_{\Gamma_2} = 0. \tag{11.2}$$

Hence, we can model four different situations:

- SS conditions (stress-free/stress-free): (10.1) and (11.1);
- SD conditions (stress-free/displacement-fixed): (10.1) and (11.2);
- DS conditions (displacement-fixed/stress-free): (10.2) and (11.1);
- DD conditions (displacement-fixed/displacement-fixed): (10.2) and (11.2).

Boundary conditions of SD and DS types are also known as mixed.

The method for sector cylinders can be used to analyze waveguides with arbitrary boundary conditions on the cylindrical surfaces and short-circuited covering by nonextensible membranes on the flat surfaces,

$$(\sigma_{\theta\theta})_{\Gamma_\pm} = (u_r)_{\Gamma_\pm} = (u_z)_{\Gamma_\pm} = (\varphi)_{\Gamma_\pm} = 0. \tag{12}$$

For circular cylinders with sector cut (CS-waveguides), we consider two boundary problems: (8.1), (9), and (12) for the stress-free cylindrical surface and (8.2), (9), and (12) for the displacement-fixed cylindrical surface.

Finally, for hollow cylinders with sector cut (HS-waveguides), also four types of boundary problems could be considered: SS, SD, DS, or DD conditions with (12). Other boundary conditions (see, for example, [54]) could be applied in this model as well.

4 Frequency equations

The frequency equations for the problems under consideration are obtained in a form of functional determinants being equal to zero (nontrivial solutions of the systems of equations). The order of the determinants depends on the type of waveguide cross-section, and the elements depend on the type of boundary conditions.

4.1 Circular cylinders

For the cylinders of circular cross-section, the metaharmonic functions χ_j are of the following form:

$$\begin{aligned} \chi_j{}^{(r,\theta)} &= \sum_{n=1}^{\infty} A_{jn} J_n(\gamma_j r) \cos n\theta \quad (j = \overline{1,3}), \\ \chi_4{}^{(r,\theta)} &= \sum_{n=1}^{\infty} A_{4n} J_n(\gamma_4 r) \sin n\theta; \end{aligned} \tag{13}$$

where A_{jn} are amplitude constants, and Bessel functions of the first kind J are of the integer index n—the circumferential wave number.

After substitution of (13) into (6) and (5), boundary conditions result for each value of $n = 1, 2, 3\ldots$ in a system of four linear homogeneous algebraic equations in the unknown coefficients A_{jn}. A nontrivial solution of this system is when its main determinant equals zero,

$$\begin{vmatrix} \Delta_{11} & \Delta_{12} & \Delta_{13} & \Delta_{14} \\ \Delta_{21} & \Delta_{22} & \Delta_{23} & \Delta_{24} \\ \Delta_{31} & \Delta_{32} & \Delta_{33} & \Delta_{34} \\ \Delta_{41} & \Delta_{42} & \Delta_{43} & \Delta_{44} \end{vmatrix} = 0. \tag{14}$$

This is the frequency equation of the system. The expressions for $\Delta_{ij} = \Delta_{ij}^{(n)}(\Omega, k)$ $(i, j = \overline{1,4})$ are given in the Appendix.

4.2 Hollow cylinders

For the hollow piezoelectric cylinders, the metaharmonic functions χ_j have a more general form

$$\begin{aligned} \chi_j(r,\theta) &= \sum_{n=1}^{\infty} \left(A_{jn} J_n(\gamma_j r) + B_{jn} Y_n(\gamma_j r)\right) \cos n\theta \quad (j = \overline{1,3}), \\ \chi_4(r,\theta) &= \sum_{n=1}^{\infty} \left(A_{4n} J_n(\gamma_4 r) + B_{4n} Y_n(\gamma_4 r)\right) \sin n\theta. \end{aligned} \tag{15}$$

Some authors [19,20] considered the dispersion equations for circular cylindrical waveguides as a special case of the equations for hollow cylinders (without the coefficients B_{jn} and Bessel functions of the second kind Y).

We obtain a system of eight linear homogeneous algebraic equations for each value of $n = 1, 2, 3\ldots$ The frequency equation is found by setting the determinant of the eighth order equal to zero:

$$\begin{vmatrix} \Delta_{1111} & & & \Delta_{1211} & & \\ & \ddots & & & \ddots & \\ & & \Delta_{1144} & & & \Delta_{1244} \\ \Delta_{2111} & & & \Delta_{2211} & & \\ & \ddots & & & \ddots & \\ & & \Delta_{2144} & & & \Delta_{2244} \end{vmatrix} = 0 \tag{16}$$

where $\Delta_{lmij} = \Delta_{lmij}^{(n)}(\Omega, k)$ $(l, m = 1, 2;\ \ i, j = \overline{1,4})$ are described in the Appendix.

4.3 Circular sector cylinders

For the cylinders of circular cross-section with sector cut, we use the following form of functions χ_j [53]:

$$\begin{aligned} \chi_j{}^{(r,\theta)} &= \sum_{n=0}^{\infty} A_{jn} J_{\lambda_n}(\gamma_j r) \cos \lambda_n \theta \quad (j = \overline{1,3}), \\ \chi_4{}^{(r,\theta)} &= \sum_{n=0}^{\infty} A_{4n} J_{\lambda_n}(\gamma_4 r) \sin \lambda_n \theta, \end{aligned} \tag{17}$$

which are similar to (13), but now the index of Bessel functions is not an integer,

$$\lambda_n = \frac{(2n+1)\pi}{2\alpha} \quad (n = 0, 1, 2 \ldots). \tag{18}$$

Hence,

$$\cos \frac{(2n+1)\pi}{2\alpha} \theta \Big|_{\theta=\pm\alpha} = \cos\left(\frac{\pi}{2} \pm \pi n\right) = 0; \tag{19}$$

and since $\sigma_{\theta\theta}, u_r, u_z$, and φ are expressed in terms of cosine functions, this choice of λ_n ensures that the boundary conditions (12) are satisfied directly.

The expressions for u_r and u_θ include terms $r^{-1} J_{\lambda_n}(\gamma_j r)$, which have singularities at $r = 0$ when $\lambda_n - 1 < 0$. Therefore, when the angular measure α of a CS-waveguide is larger than $\frac{\pi}{2}$, the permitted values of n are $1, 2, 3 \ldots$

Boundary conditions of the cylindrical surface result into the frequency equation in the form of the fourth-order determinant with elements obtained from Δ_{ij} for the case of a circular waveguide without cuts by substitution $n \to \lambda_n$.

4.4 Hollow sector cylinders

Finally, for the hollow cylinders with sector cut, the metaharmonic functions χ_j have the following form:

$$\begin{aligned} \chi_j(r,\theta) &= \sum_{n=0}^{\infty} \left(A_{jn} J_{\lambda_n}(\gamma_{jr}) + B_{jn} Y_{\lambda_n}(\gamma_j r)\right) \cos \lambda_n \theta \quad (j = \overline{1,3}), \\ \chi_4(r,\theta) &= \sum_{n=0}^{\infty} \left(A_{4n} J_{\lambda_n}(\gamma_4 r) + B_{4n} Y_{\lambda_n}(\gamma_4 r)\right) \sin \lambda_n \theta; \\ \lambda_n &= \frac{(2n+1)\pi}{2\alpha} \quad (n = 0, 1, 2 \ldots). \end{aligned} \tag{20}$$

Again, the boundary conditions on the flat surfaces are satisfied directly, and the frequency equation of the system is the determinant of the eighth order equal to zero. In a similar manner, we obtain its elements from Δ_{lmij} for the case of a hollow cylinder without cuts by replacing $n \to \lambda_n$.

5 Numerical results and discussion

In the previous Section, the frequency equations were obtained from the boundary conditions in the form of fourth- and eight-order determinants. In this Section, numerical results for all cylinders under consideration will be presented and discussed. These waveguides are composed of a PZT-5A material whose properties are given in [2,44,47].

In order to obtain the real and imaginary branches of dispersion curves, the fast and "smart" bisection method was used, which decreases the interval and increases the precision when the roots are very close to each other, and hence, it does not miss them. To verify the algorithm, some plots calculated by it for circular

cylinders (fourth-order determinants) were compared with the graphs obtained by the method described by Honarvar et al. [55], where the dispersion curves are obtained by a two-dimensional cut of a three-dimensional plot in the velocity–frequency plane. Both techniques have produced identical curves.

Two characteristics that play an important role when studying wave propagation are phase and group velocities. Each propagating wave has phase velocity $c_p = \frac{\Omega}{k}$ and group velocity $c_g = \frac{\partial \Omega}{\partial k} = -\frac{F_k(\Omega,k)}{F_\Omega(\Omega,k)}$. Since there is no attenuation, group velocity represents the rate at which the energy of waves is transported. All phase and group velocities from one mode at high-frequency approach some constant. These plots are also presented below for some cases, and to evaluate the group velocity, the differentials $F_k(\Omega, k)$ and $F_\Omega(\Omega, k)$ were calculated numerically. The distributions of dispersion curves, phase, and group velocities are presented in the commonly used [18–20,23,26,30–33,48,54,55] form of dimensionless frequency versus dimensionless wavenumber and dimensionless velocity versus dimensionless frequency, respectively. The angular frequency Ω is normalized in the following way:

$$\Omega = \sqrt{\frac{\rho}{c_*}} R_* \omega; \tag{21}$$

where R_* and c_* are the normalizing factors for the units of length and elastic constants, respectively.

5.1 Circular cylinders

Dispersion curves of flexural waves with $n = 1$ for the circular waveguide with stress-free surface are shown in Fig. 2a. The first mode has zero cutoff frequency, and the fourth mode has a negative slope (the so-called backward waves when the phase and group velocities have different signs). A similar behavior of the dispersion curves is demonstrated by Shatalov et al. ([48], Figs. 1 and 4). Nonpropagating modes with purely imaginary values of k form almost vertical lines in the left part of the spectrum and sometimes come very close to each other in the inflection points, which is common for piezoelectric structures.

Figure 2b shows phase velocity curves in the same range of the dimensionless frequency Ω. The solid and dash-dot horizontal lines represent the velocities of Rayleigh surface c_R and shear elastic waves c_S, respectively. It can be seen from Fig. 2b that after some frequency the phase velocities of all the waves from one mode become almost constant (modes have negligible dispersion). In the circular cylinder with stress-free boundary, phase velocities of the waves from the first mode are approaching the velocity of Rayleigh waves in the high-frequency limit, and waves from the other modes are transformed into shear elastic waves. The same effect is described in [30] for cylinders of cubic anisotropy. Backward waves in the fourth mode can also be noted from the group velocity curves in Fig. 2c.

One of the main questions of the study is how to control the spectrum and characteristics of elastic waves in the waveguide. One may choose different material or apply boundary conditions on the cylindrical surface. It is not always possible, but it is the only way to change wave characteristics for circular cylinders (of course, a change in the cylinder radius will result in a wavelength change, but in the dimensionless coordinates, the spectrum will be the same).

The problem of wave propagation in piezoelectric cylinders was analyzed for different materials, and types of mechanical and electric boundary conditions and comparisons can be found in the literature [48,54]. Dispersion curves for the cylinder with displacement-fixed surface are presented in Fig. 3a. In this case, no mode has zero cutoff frequency, and backward waves occur in the first and fifth modes. Again, as in the case of a stress-free boundary, the first and second, and fifth and sixth modes unite in the imaginary part of the spectrum. Phase and group velocity curves are illustrated in Fig. 3b and c, respectively. As is well-known, for the case of cylinders with displacement-fixed boundary, the asymptote for the phase velocities of all waves is the velocity of shear waves.

5.2 Hollow cylinders

Figures 4 and 5 illustrate the propagation of electroelastic waves in hollow piezoelectric cylinders. All four types of boundary conditions discussed in Sect. 3 are applied on the surfaces of the cylinder with inner radius $R_1 = 0.5R_2$: SS conditions (Fig. 4a), SD conditions (Fig. 4b), DS conditions (Fig. 4c), and DD conditions (Fig. 4d). Again, as in the case of circular cylinders, the mode with zero cutoff frequency is present only for the case of stress-free (SS) boundaries. Fixing the outer surface of the cylinder (SD) leads to the changes in

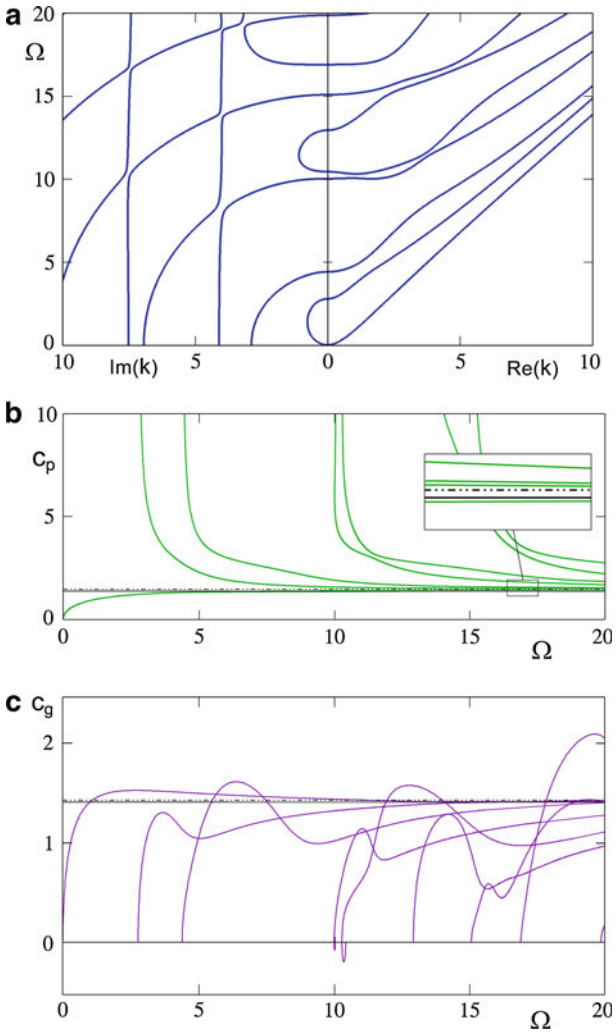

Fig. 2 Circular cylinder with stress-free surface, $n = 1$. **a** Dispersion curves, **b** phase velocities, **c** group velocities

the behavior of the lowest modes. The second and third modes come very close to each other in the inflection point near $k = 2.7$ but, of course, do not intersect. The phenomenon of backward waves is clearly observed for the first mode of the cylinder with fixed inner surface (DS). In the waveguides with both fixed surfaces (DD), the loop in the imaginary part of the spectrum is the imaginary part of the first and second modes linked to them by a complex branch [18,23].

For hollow cylinders, there is another way to control the wave propagation in addition to choosing different material and boundary conditions: changing the thickness (ratio of inner-outer radii). Dispersion curves for the thick waveguide ($R_1 = 0.1R_2$ so the thickness is 9 times bigger than the inner radius) with stress-free surfaces are shown in Fig. 5a. Three lowest modes of this spectrum are found to be similar to the modes of the spectrum for a circular cylinder (Fig. 2a). A further increase of the thickness results in the changes in the fourth and next modes, which become more similar to the case of the circular cylinder. On the contrary, curves for the three relatively thin hollow cylinders ($R_1 = 0.7R_2$, $R_1 = 0.8R_2$ and $R_1 = 0.9R_2$) shown in Fig. 5b differ quite substantially from the curves for the solid and relatively thick hollow cylinders. The difference increases with the decrease in the cylinder thickness.

Figures 6a and b show the distributions of phase and group velocities, respectively, for the cylinder with inner radius $R_1 = 0.5R_2$ and SS boundary conditions (Fig. 4a). The high-frequency limit of the first and second modes is the Rayleigh surface wave velocity (solid horizontal line). For the third and next modes, the high-frequency limit is the velocity of shear elastic waves (dash-dot horizontal line). Plots of the group velocity

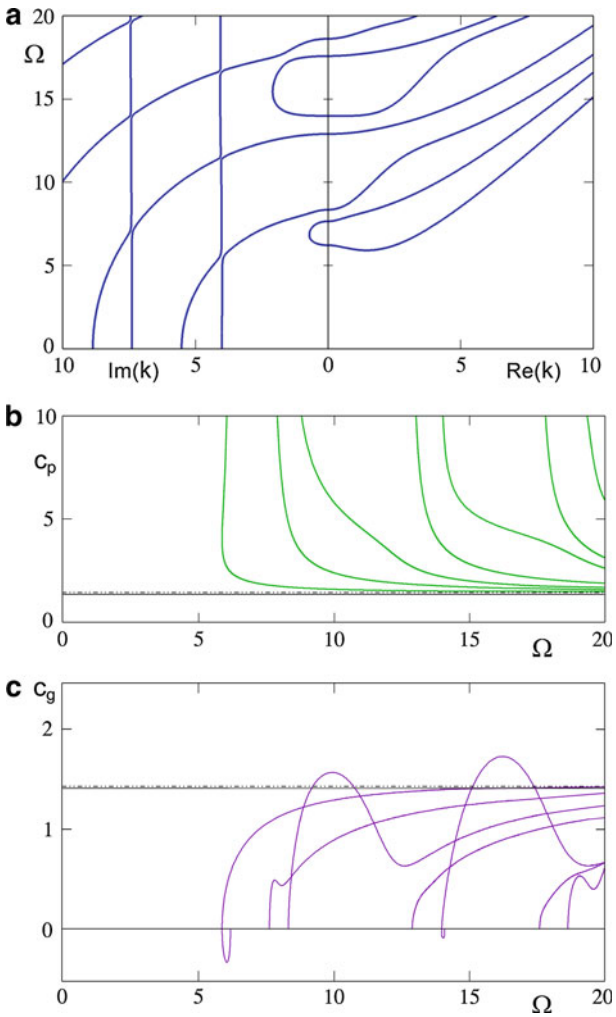

Fig. 3 Circular cylinder with displacement-fixed surface, $n = 1$. **a** Dispersion curves, **b** phase velocities, **c** group velocities

curves are very useful for problems related to the backward waves, for example, their absence in the lowest modes of elastic waves with $n = 1$ in the stress-free cylinder can be easily noted from Fig. 6b.

5.3 Circular sector cylinders

Two partial dispersion spectra for the circular sector cylinders of angular measure $\alpha = 0.25\pi$ (quadrant) and $\alpha = 0.5\pi$ (semicircle) with $n = 0$ and stress-free cylindrical surface are illustrated in Fig. 7. The first mode of a semicircle waveguide has zero cutoff frequency while waveguides with another angular measure do not have such modes. Figure 8a shows the real branches for the four sector cylinders of angular measure $\alpha = 0.25\pi$, $\alpha = 0.3\pi$, $\alpha = 0.4\pi$, and $\alpha = 0.5\pi$. It can be readily seen that increasing α leads to a decrease of the curve positions. When the step of the change of α is very small, the variation of curves is small, too. Therefore, we can obtain the wave with specific frequency and length (a point in the Ω-k plot) in comparatively wide limits by changing the angular measure of the waveguide. The regions of possible changes in the lowest five curves are shown in Fig 8b. The lower and upper limits for α were chosen to be 0.25π and 0.5π, respectively, so, taking into account that frequencies are monotonically decreasing, the boundaries of the regions are the curves from Fig. 7. The right bottom part of the figures is a region of low-frequency short waves that do not propagate in the waveguides under consideration. The first mode in Fig. 8b has a comparatively smaller change limit than the other ones at moderate values of the dimensionless wavenumber.

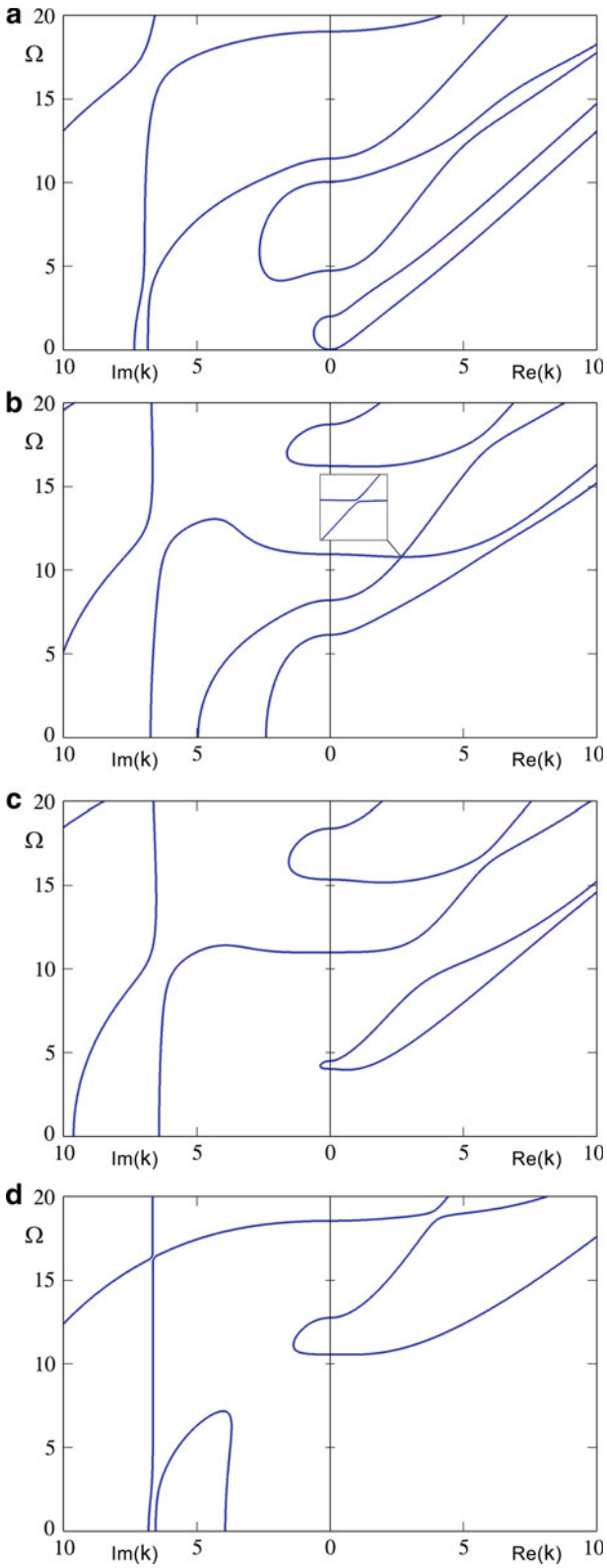

Fig. 4 Dispersion curves for hollow cylinders with different boundary conditions, $R_1 = 0.5R_2$, $n = 1$. **a** Free/free, **b** free/fixed, **c** fixed/free, **d** fixed/fixed

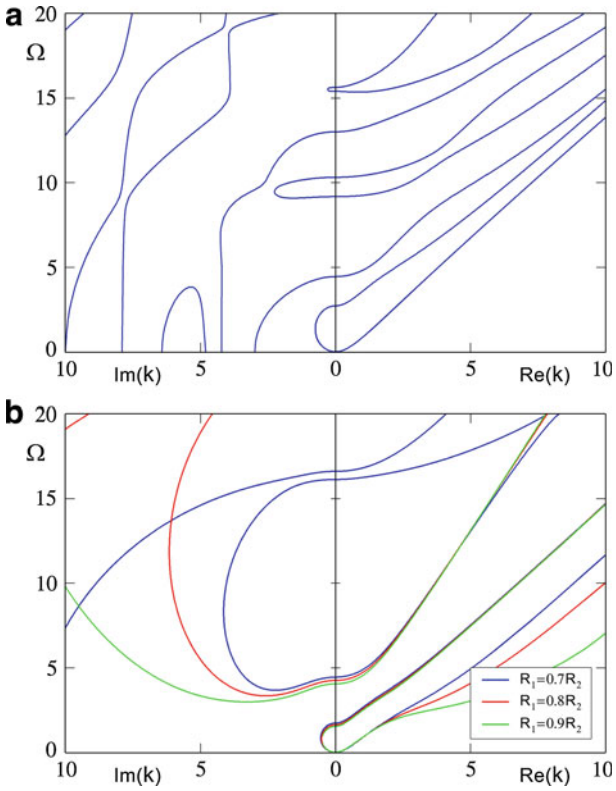

Fig. 5 Dispersion curves for hollow cylinders with stress-free surfaces, $n = 1$. **a** $R_1 = 0.1R_2$, **b** $R_1 = 0.7R_2$, $R_1 = 0.8R_2$, $R_1 = 0.9R_2$

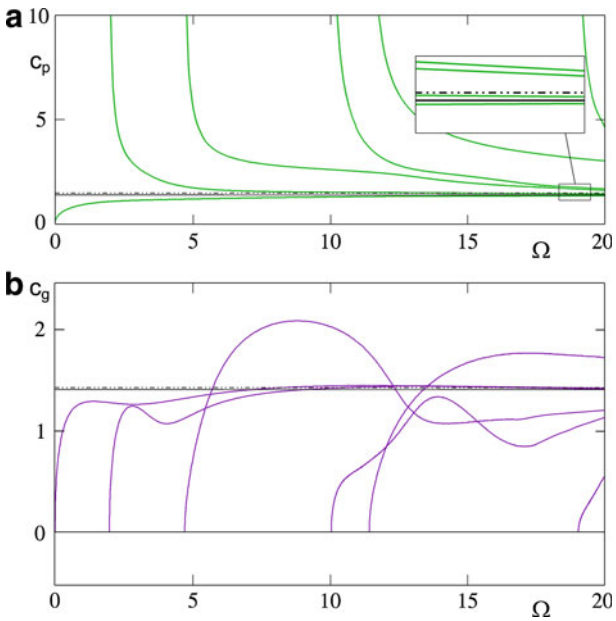

Fig. 6 Hollow cylinder with stress-free surfaces, $R_1 = 0.5R_2$, $n = 1$. **a** Phase velocities, **b** group velocities

The same situation is observed for the spectra with $n = 1$ for the cylinders of angular measure $\alpha \in [0.5\pi; 0.8\pi]$. As seen in Fig. 9, the angular measure of the waveguide affects significantly the wave quantitative characteristics. Frequencies of all modes for the waves with the same values of n decrease with the increase in α, and all curves can change in comparatively wide limits. This could be explained by the significant influence of the cross-section geometry rather than the piezoceramic material on wave propagation. Many

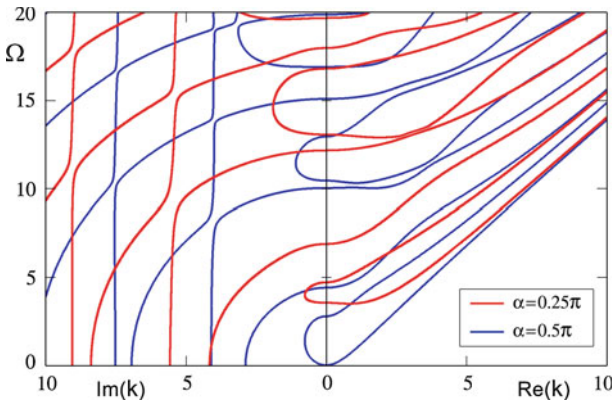

Fig. 7 Dispersion curves for circular sector cylinders with stress-free surface, $\alpha = 0.25\pi$ and $\alpha = 0.5\pi$, $n = 0$

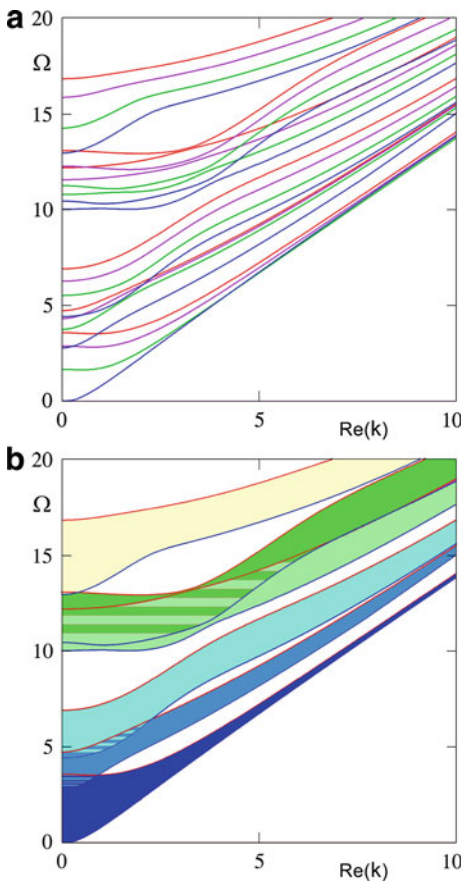

Fig. 8 Circular sector cylinders with stress-free surface, $n = 0$. **a** Real parts of the curves for $\alpha = 0.25\pi, \alpha = 0.3\pi, \alpha = 0.4\pi, \alpha = 0.5\pi$. **b** Regions of change for $\alpha \in [0.25\pi; 0.5\pi]$

comparisons have been made in the literature for canonical circular cylinders, for example, [40,48] or [30,33] for nonpiezoelectric waveguides. It also follows from Fig. 9 that the first and second modes are less sensitive to the angular measure of sector cut than the higher modes.

Phase velocities, as in the case of waveguides without cut, are clearly dependent on the boundary conditions. For the cylinders with stress-free boundary, the phase velocity of a Rayleigh surface wave is the asymptotic value for the velocities of the first modes. The velocities of the second and other modes (and of all modes for the cylinders with fixed boundary), as expected, tend to the shear wave velocity at high frequencies.

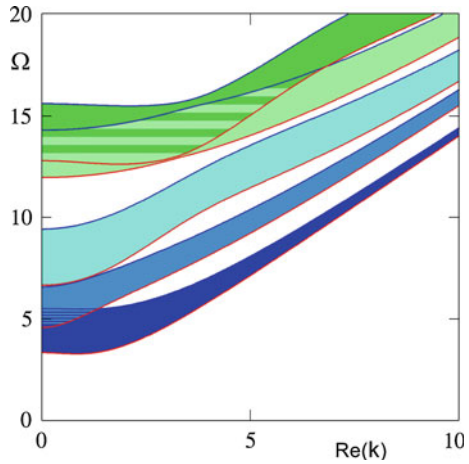

Fig. 9 Regions of change for circular sector cylinders with stress-free surface when $\alpha \in [0.5\pi; 0.8\pi]$, $n = 1$

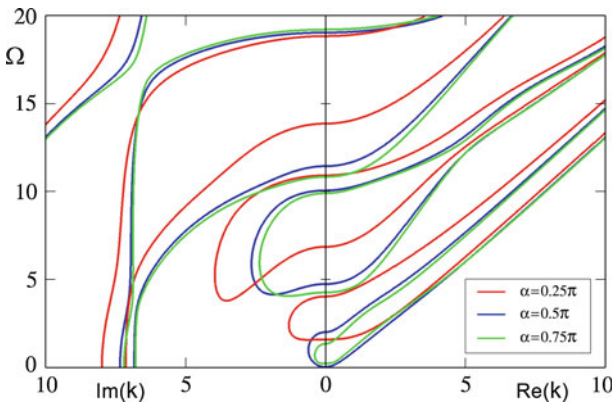

Fig. 10 Dispersion curves for hollow sector cylinders with stress-free surfaces, $R_1 = 0.5R_2, \alpha = 0.25\pi, \alpha = 0.5\pi$, and $\alpha = 0.75\pi, n = 0$

5.4 Hollow sector cylinders

Figure 10 illustrates the real and imaginary branches of dispersion curves in cylinders with stress-free cylindrical surfaces, inner radius $R_1 = 0.5R_2$, and three different angular measures $\alpha = 0.25\pi, \alpha = 0.5\pi, \alpha = 0.75\pi$. These curves are plotted analogously to those for the circular sector cylinders, and a comparison can be made. As in the previous case, frequencies of the lowest modes decrease when α increases from 0.25π to 0.5π. For $\alpha \in [0.5\pi; 0.75\pi]$, the situation is more complex, for example, different parts of the first and third modes become lower or higher. We can also observe that the dispersion curves for the case of $\alpha = 0.25\pi$ differ quite substantially from the curves for the two other values of angular measure. Therefore, in this case, variation of cross-section geometry is more essential in the range of 0.25π to 0.5π. It should be also noted that there are no backward waves for the lowest modes.

In the next step, we have studied the possibilities to control wave propagation by changing the thickness of the cylinders. The results of the simulations performed for the four different ratios of inner-outer radii ($R_1 = 0.2R_2$, $R_1 = 0.4R_2$, $R_1 = 0.6R_2$ and $R_1 = 0.8R_2$) and angular measure $\alpha = 0.75\pi$ are plotted in Fig. 11. Comparison of these curves reveals that in low as well as high-frequency range, the thickness parameter affects strongly the spectra. Cutoff frequencies of the first modes are small, but bigger than zero. An increase of the inner radius results in the larger decrease of the first mode at moderate values of the dimensionless wavenumber; however, it tends to the asymptote with the increase in the wavenumber. Figure 12 shows the regions of change for the three lowest modes when $\alpha \in [0.25\pi; 0.75\pi]$, $R_1/R_2 \in [0.2; 0.8]$. The influence of both factors is more noticeable than for the case of hollow cylinders (variable thickness) or circular sector cylinders (variable angular measure). However, as pointed out in the previous subsections, the high-frequency short-wave limit is determined by the boundary conditions.

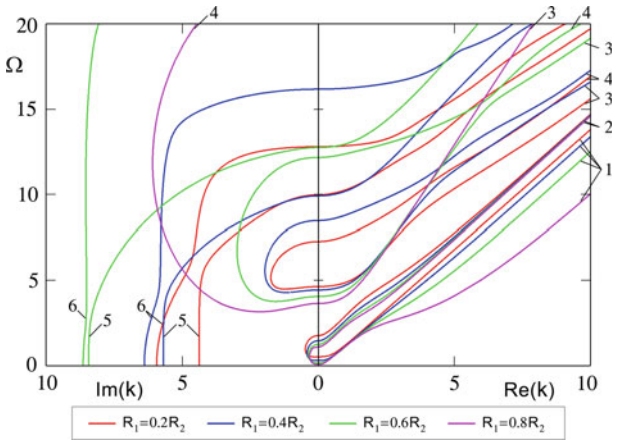

Fig. 11 Dispersion curves for hollow sector cylinders with stress-free surfaces, $\alpha = 0.75\pi$, $R_1 = 0.2R_2$, $R_1 = 0.4R_2$, $R_1 = 0.6R_2$ and $R_1 = 0.8R_2$, $n = 0$

5.5 Dependence on the cross-section area

Another question that arises from the analysis of the influence of geometric factors is how does wave propagation depend on the area of waveguide cross-section. If we have a given value of the area (amount of piezoceramic material), we can choose the most suitable form of cross-section from those under consideration. The formulas for the cross-sectional area of circular and hollow sector waveguides are $S_c = \alpha R^2$ and $S_h = \alpha \left(R_2^2 - R_1^2\right)$, respectively (the formulas for the waveguides without cuts are the same with π instead of α).

According to Eqs. (21), there is an inversely proportional relationship between the angular frequency ω and the normalizing factor R_* (which is chosen to be equal to the outer radius)

$$\omega = \sqrt{\frac{c_*}{\rho}} \frac{\Omega}{R_*}; \tag{22}$$

since the area of a circle is dependent on the square of the radius, the angular frequency ω is inversely proportional to the square root of the area $\sqrt{S}$.

Cutoff frequencies in the form of relative frequency versus relative cross-section area are shown in Fig. 13. The first mode for the circular cylinders has zero cutoff frequency, and the second cutoff frequency is represented in Fig. 13 in the line $\widetilde{\omega} = 1/\sqrt{S}$. Comparison between these results and the first and second modes of sector cylinders ($\alpha = S\pi/4$, *squares* and *circles*, respectively) shows noticeable differences. In general, the form of a waveguide cross-section has a significant effect on the dispersion behavior of elastic waves.

6 Conclusions

Studies of the dynamic behavior of piezoelectric cylinders are of particular importance from both theoretical and practical points of view. Although the necessary properties may be obtained by the selection of appropriate piezoceramic material, however sometimes it is difficult to vary material characteristics in the required range. Therefore, variation of cross-section geometry and boundary conditions plays an important role in waveguide dynamics. In this paper, we have compared the wave propagation in the piezoelectric cylinders with the four types of cross-section and provided the dispersion relations with no restrictions on frequency and wavenumber. The numerical results include dispersion curves plots accompanied by phase/group velocity graphs for waveguides with different cross-section geometry. The values of cylinder thickness and angular measure have a significant influence on the frequency spectra both qualitatively and quantitatively. A mode with zero cutoff frequency (starting from point $(0, 0)$) is present in spectra of flexural waves with $n = 1$ in circular and hollow cylinders, and in spectra of waves with $n = 0$ in semi-circular and semi-hollow cylinders. This is consistent with the other observations on cylindrical waveguides [18–20,23,33,48,54]. Waves with

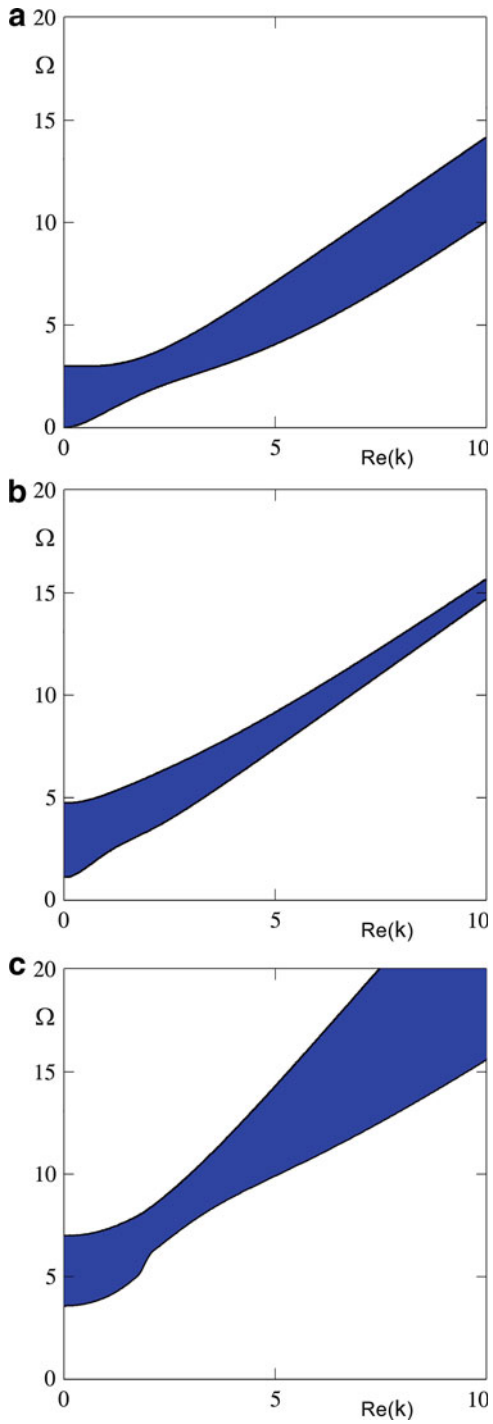

Fig. 12 Regions of change for hollow sector cylinders with stress-free surfaces when $\alpha \in [0.25\pi; 0.75\pi]$, $R_1/R_2 \in [0.2; 0.8]$, $n = 0$. **a** 1st mode, **b** 2nd mode, **c** 3rd mode

negative group velocity were observed in some spectra at a range of small wavenumbers. A brief analysis of the dependence of wave propagation characteristics on the area of waveguide cross-section is also carried out, and high-frequency short-wave localization is discussed.

The results of this study clearly illustrate the possibility to obtain necessary wave characteristics of circular and hollow piezoelectric cylinders by changing the angular measure of sector cut and the ratio of inner-outer radii. The effect of boundary conditions on the cylindrical surfaces is also studied for some cases, and the

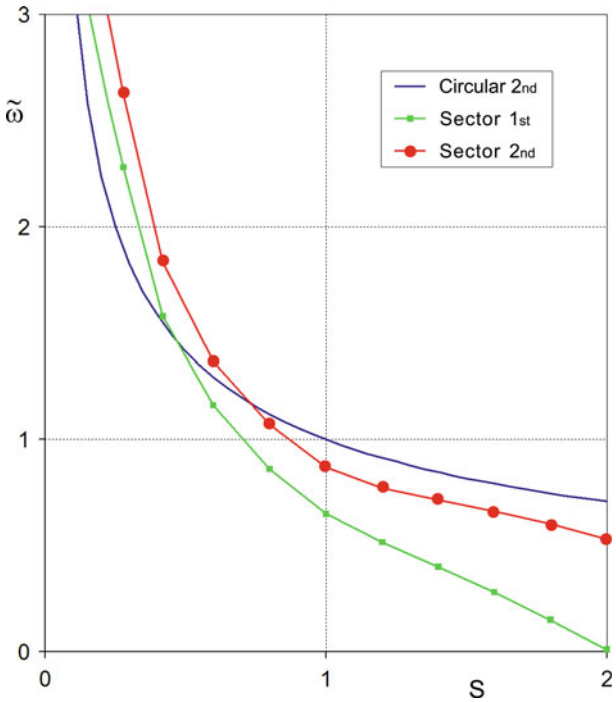

Fig. 13 Cutoff frequencies dependence on the cross-section area: circular cylinder ($n = 1$) and sector circular cylinder ($n = 0$)

modes are found to be sensitive to the nature of mechanical and electric boundary conditions. The variation of the cross-section geometry is considered to be another mechanism to control the dynamic behavior of waveguides. Since these results are obtained from the exact solution of the problem, some of them could be used as reference data for applying approximate methods to the problems of wave propagation in piezoelectric waveguides.

Appendix

The elements of the determinant (14) for the case of stress-free boundary conditions (8.1) are as follows:

$$
\begin{aligned}
\Delta_{1j} &= \beta_{1j}\cdot\left(\frac{2c_{66}\gamma_j}{R}J_{n+1}(\gamma_j R)-c_{11}\gamma_j^2 J_n(\gamma_j R)+\frac{2c_{66}n\,(n-1)}{R^2}J_n(\gamma_j R)\right)\\
&\quad +ikc_{13}\beta_{2j}J_n(\gamma_j R)-ike_{31}\beta_{3j}J_n(\gamma_j R)\quad (j=\overline{1,3}),\\
\Delta_{14} &= \frac{2c_{66}n}{R}\left(\frac{n-1}{R}J_n(\gamma_4 R)-\gamma_4 J_{n+1}(\gamma_4 R)\right),\\
\Delta_{2j} &= \beta_{1j}\frac{2c_{66}n}{R}\left(\gamma_j J_{n+1}(\gamma_j R)-\frac{n-1}{R}J_n(\gamma_j R)\right)\quad (j=\overline{1,3}),\\
\Delta_{24} &= -2c_{66}\left(\frac{n\,(n-1)}{R^2}J_n(\gamma_4 R)+\frac{\gamma_4}{R}J_{n+1}(\gamma_4 R)-\frac{\gamma_4^2}{2}J_n(\gamma_4 R)\right),\\
\Delta_{3j} &= \left(c_{44}\left(\beta_{1j}ik+\beta_{2j}\right)-e_{15}\beta_{3j}\right)\left(\frac{n}{R}J_n(\gamma_j R)-\gamma_j J_{n+1}(\gamma_j R)\right)\quad (j=\overline{1,3}),\\
\Delta_{34} &= \frac{ikc_{44}n}{R}J_n(\gamma_4 R);
\end{aligned}
\tag{A.1}
$$

and for the case of displacement-fixed boundary conditions (8.2):

$$\begin{aligned}
\Delta_{1j} &= \beta_{1j}\left(\frac{n}{R}J_n(\gamma_j R) - \gamma_j J_{n+1}(\gamma_j R)\right) \quad (j=\overline{1,3}),\\
\Delta_{14} &= \frac{n}{R}J_n(\gamma_4 R),\\
\Delta_{2j} &= -\beta_{1j}\frac{n}{R}J_n(\gamma_j R) \quad (j=\overline{1,3}),\\
\Delta_{24} &= -\left(\frac{n}{R}J_n(\gamma_4 R) - \gamma_4 J_{n+1}(\gamma_4 R)\right),\\
\Delta_{3j} &= \beta_{2j}J_n(\gamma_j R) \quad (j=\overline{1,3}),\\
\Delta_{34} &= 0.
\end{aligned} \tag{A.2}$$

And the elements of the last row Δ_{4j} for the case of close circuit boundary conditions (9) are as follows:

$$\begin{aligned}
\Delta_{4j} &= \beta_{3j}J_n(\gamma_j R) \quad (j=\overline{1,3}),\\
\Delta_{44} &= 0.
\end{aligned} \tag{A.3}$$

The elements of the determinant (16) for a hollow cylinder could be obtained from (A.1–3) by the following rules:

$$\begin{aligned}
\Delta_{11ij} &= \Delta_{ij}\big|_{R=R_1}, \quad \Delta_{12ij} = \Delta_{ij}\big|_{R=R_1,\ J\leftrightarrow Y},\\
\Delta_{21ij} &= \Delta_{ij}\big|_{R=R_2}, \quad \Delta_{22ij} = \Delta_{ij}\big|_{R=R_2,\ J\leftrightarrow Y} \quad (i,j=\overline{1,4}).
\end{aligned} \tag{A.4}$$

References

1. Tiersten, H.F.: Linear Piezoelectric Plate Vibrations. Plenum, New York (1969)
2. Berlincourt, D.A., Curran, D.R., Jaffe, H.: Piezoelectric and piezomagnetic materials and their functions in transducers. In: Mason, W.P. (ed.) Physical Acoustics: Principles and Methods, 1A, Academic Press, New York (1964)
3. Maugin, G.A.: Continuum Mechanics of Electromagnetic Solids. North-Holland, Amsterdam (1988)
4. Parton, V.Z., Kudryavtsev, B.A.: Electromagnetoelasticity. Gordon and Breach, New York (1988)
5. Uchino, K.: Piezoelectric Actuators and Ultrasonic Motors. Kluwer Academic Publishers, Boston (1996)
6. Uchino, K.: Piezoelectric ultrasonic motors: overview. Smart Mater. Struct. **7**, 273–285 (1998)
7. Benes, E., Groschl, M., Burger, W., Schmid, M.: Sensors based on piezoelectric resonators. Sens. Actuators A **48**, 1–21 (1995)
8. Drinkwater, B.W., Wilcox, P.D.: Ultrasonic arrays for non-destructive evaluation: a review. NDT&E Int. **39**, 525–541 (2006)
9. Kim, J.O., Lee, J.G.: Dynamic characteristics of piezoelectric cylindrical transducers with radial polarization. J. Sound Vib. **300**, 241–249 (2007)
10. Vashishth, A.K., Gupta, V.: Wave propagation in transversely isotropic porous piezoelectric materials. Int. J. Solids Struct. **46**, 3620–3632 (2009)
11. Kapuria, S., Kumari, P., Nath, J.K.: Efficient modeling of smart piezoelectric composite laminates: a review. Acta Mech. **214**, 31–48 (2010)
12. Guo, S.H.: The thermo-electromagnetic waves in piezoelectric solids. Acta Mech. **219**, 231–240 (2011)
13. Morse, R.W.: Compressional waves along an anisotropic circular cylinder having hexagonal symmetry. J. Acoust. Soc. Am. **26**, 1018–1021 (1954)
14. Gazis, D.C.: Three dimensional investigation of the propagation of waves of hollow circular cylinder. Part I: Analytical foundation, Part II: numerical results. J. Acoust. Soc. Am. **31**, 568–578 (1959)
15. Mindlin, R.D., McNiven, H.D.: Axially symmetric waves in elastic rods. J. Appl. Mech. **27**, 145–151 (1960)
16. Pao, Y.H., Mindlin, R.D.: The dispersion of flexural waves in an elastic circular cylinder. J. Appl. Mech. **27**, 513–520 (1960)
17. Pao, Y.H.: The dispersion of flexural waves in an elastic circular cylinder, part II. J. Appl. Mech. **29**, 61–64 (1962)
18. Onoe, M.A., McNiven, H.D., Mindlin, R.D.: Dispersion of axially symmetric waves in elastic rods. J. Appl. Mech. **29**, 729–734 (1962)
19. Mirsky, I.: Wave propagation in transversely isotropic circular cylinders, Part I: theory, Part II: numerical results. J. Acoust. Soc. Am. **37**, 1016–1026 (1965)
20. Meeker, T.R., Meitzler, A.H. : Guided wave propagation in elongated cylinders and plates. In: Mason, W.P. (ed.) Physical Acoustics: Principles and Methods, 1A, Academic Press, New York (1964)
21. McNiven, H.D., McCoy, J.J.: Vibration and wave propagation in rods. In: R.D. Mindlin and Applied Mechanics. Pergamon, New York (1974)
22. Thurston, R.N.: Elastic waves in rods and clad rods. J. Acoust. Soc. Am. **64**, 1–37 (1978)
23. Zemanek, J.: An experimental and theoretical investigation of elastic wave propagation in a cylinder. J. Acoust. Soc. Am. **51**, 265–283 (1972)
24. Meleshko, V.V., Bondarenko, A.A., Dovgiy, S.A., Trofimchuk, A.N., van Heijst, G.J.F.: Elastic waveguides: history and the state of the art. J. Math. Sci. **162**, 99–120 (2009)

25. Tsai, Y.M.: Longitudinal motion of a transversely isotropic hollow cylinder. J. Press. Vessel Technol. **113**, 585–589 (1991)
26. Berliner, M.J., Solecki, R.: Wave propagation in fluid-loaded, transversely isotropic cylinders, Part I: Analytical formulation, Part II: numerical results. J. Acoust. Soc. Am. **99**, 1841–1853 (1996)
27. Andrianov, I., Awrejcewicz, J.: Simplified formula for the vibration frequency of circular cylinders. J. Sound Vib. **262**, 198–200 (2003)
28. Damljanovic, V., Weaver, R.L.: Propagating and evanescent elastic waves in cylindrical waveguides of arbitrary cross section. J. Acoust. Soc. Am. **115**, 1572–1581 (2004)
29. Grigorenko, A.Ya., Vlaikov, G.G.: Investigation of the static and dynamic behaviour of anisotropic cylindrical bodies with noncircular cross-section. Int. J. Solids Struct. **41**, 2781–2798 (2004)
30. Elmaimouni, L., Lefebvre, J.E., Zhang, V., Gryba, T.: A polynomial approach to the analysis of guided waves in anisotropic cylinders of infinite length. Wave Motion **42**, 177–189 (2005)
31. Puckett, D., Peterson, M.L.: A semi-analytical model for predicting multiple propagating axially symmetric modes in cylindrical waveguides. Ultrasonics **43**, 197–207 (2005)
32. Hayashi, T., Tamayama, C., Murase, M.: Wave structure analysis of guided waves in a bar with an arbitrary cross-section. Ultrasonics **44**, 17–24 (2006)
33. Honarvar, F., Enjilela, E., Sinclair, A.N., Mirnezami, S.A.: Wave propagation in transversely isotropic cylinders. Int. J. Solids Struct. **44**, 5236–5246 (2007)
34. Fan, Z., Lowe, M.J.S., Castaings, M., Bacon, C.: Torsional waves propagation along a waveguide of arbitrary cross section immersed in a perfect fluid. J. Acoust. Soc. Am. **124**, 2002–2010 (2008)
35. Ponnusamy, P., Rajagopal, M.: Wave propagation in a transversely isotropic solid cylinder of arbitrary cross-sections immersed in fluid. Eur. J. Mech. A **29**, 158–165 (2010)
36. Zhou, D., Cheung, Y.K., Lo, S.H.: 3-D vibration analysis of circular rings with sectorial cross-sections. J. Sound Vib. **329**, 1523–1535 (2010)
37. EerNisse, E.P.: Variational method for electroelastic vibration analysis. IEEE Trans. Sonics Ultrasonics **14**, 153–159 (1967)
38. Adelman, N.T., Stavsky, Y., Segal, E.: Axisymmetric vibrations of radially polarized piezoelectric ceramic cylinders. J. Sound Vib. **38**, 245–254 (1975)
39. Paul, H.S., Venkatesan, M.: Wave propagation in a piezoelectric solid cylinder of arbitrary cross section. J. Acoust. Soc. Am. **82**, 2013–2020 (1987)
40. Rajapakse, R.K.N.D., Zhou, Y.: Stress analysis of piezoceramic cylinders. Smart Mater. Struct. **6**, 169–177 (1997)
41. Wang, Q.: Axi-symmetric wave propagation in cylinder coated with a piezoelectric layer. Int. J. Solids Struct. **39**, 3023–3037 (2002)
42. Ebenezer, D.D., Ramesh, R.: Analysis of axially polarized piezoelectric cylinders with arbitrary boundary conditions on the flat surfaces. J. Acoust. Soc. Am. **113**, 1900–1908 (2003)
43. Berg, M., Hagedorn, P., Gutschmidt, S.: On the dynamics of piezoelectric cylindrical shell. J. Sound Vib. **274**, 91–109 (2004)
44. Ebenezer, D.D., Ravichandran, K., Ramesh, R., Padmanabhan, C.: Forced responses of solid axially polarized piezoelectric ceramic finite cylinders with internal losses. J. Acoust. Soc. Am. **117**, 3645–3656 (2005)
45. Bai, H., Taciroglu, E., Dong, S., Shah, A.: Elastodynamic Green's function for a laminated piezoelectric cylinder. Int. J. Solids Struct. **41**, 6335–6350 (2004)
46. Botta, F., Cerri, G.: Wave propagation in Reissner–Mindlin piezoelectric coupled cylinder with non-constant electric field through the thickness. Int. J. Solids Struct. **44**, 6201–6219 (2007)
47. Rubio, W.M., Buiochi, F., Adamowski, J.C., Silva, E.C.N.: Modeling of functionally graded piezoelectric ultrasonic transducers. Ultrasonics **49**, 484–494 (2009)
48. Shatalov, M.Y., Every, A.G., Yenwong-Fai, A.S.: Analysis of non-axisymmetric wave propagation in a homogeneous piezoelectric solid circular cylinder of transversely isotropic material. Int. J. Solids Struct. **46**, 837–850 (2009)
49. Ying, Z.G., Wang, Y., Ni, Y.Q., Ko, J.M.: Stochastic response analysis of piezoelectric axisymmetric hollow cylinders. J. Sound Vib. **321**, 735–761 (2009)
50. Sun, D., Wang, S., Hata, S., Shimokohbe, A.: Axial vibration characteristics of a cylindrical, radially polarized piezoelectric transducer with different electrode patterns. Ultrasonics **50**, 403–410 (2010)
51. Royer, D., Dieulesaint, E.: Elastic Waves in Solids vol. 1: Free and Guided Propagation, vol. 2: Generation, Acousto-Optic Interaction, Applications. Springer, New York (2000)
52. Buchwald, V.T.: Rayleigh wave in transversely isotropic media. Q. J. Mech. Appl. Math. **14**, 293–317 (1961)
53. Puzyrev, V., Storozhev, V.: Wave propagation in axially polarized piezoelectric hollow cylinders of sector cross section. J. Sound Vib. **330**, 4508–4518 (2011)
54. Wei, J.P., Su, X.Y.: Wave propagation in a piezoelectric rod of 6 mm symmetry. Int. J. Solids Struct. **42**, 3644–3654 (2005)
55. Honarvar, F., Enjilela, E., Sinclair, A.N.: An alternative method for plotting dispersion curves. Ultrasonics **49**, 15–18 (2009)